Supporting Information

Triphenylamine based conjugated microporous polymers for selective photoreduction of CO_2 into CO under visible light

Chunhui Dai,[†§] Lixiang Zhong,[‡§] Xuezhong Gong,[‡] Lei Zeng,[‡] Can Xue,[‡] Shuzhou Li[‡*] and Bin Liu[†*]

[†]Department of Chemical and Biomolecular Engineering, National University of Singapore, 4 Engineering Drive 4, Singapore 117585, Singapore

[‡]School of Materials Science and Engineering, Nanyang Technological University, 50 Nanyang Avenue, Singapore 639798, Singapore

[§]Both authors contribute equally

* Corresponding Author. E-mail address: cheliub@nus.edu.sg; lisz@ntu.edu.sg.

Materials and Characterization

Chemicals. All chemicals and were commercially available and used as received without further purification unless otherwise stated. Tris(4-bromophenyl)amine was purchased from Combi-blocks Inc. 4-Bromobenzoyl chloride was purchased from TCI Co,. LTD (Singapore). Phosphorus oxychloride and hydrazine hydrate (50-60%) were purchased from Sigma Aldrich.

Characterization of the as-prepared conjugated microporous polymers. The ^{13}C cross-polarization magic angle spinning (CP/MAS) spectra were carried out on the Bruker AVNEO 400 spectrometer. Fourier transform infrared spectroscopy with KBr tableting range from 4000 to 400 cm^{-1} were measured by a Bio-Rad FTS-3500 ARX FTIR spectrometer. C, H, N elemental analysis of the polymers were performed on a Elementar vario MICRO cube. The palladium and copper

contents in the polymer networks were measured by inductive coupled plasma (iCAP6200DUO ICP-OES Spectrometer). The powder X-ray diffraction (PXRD) patterns were measured on a Bruker D8 Advance diffractometer (Cu Kα X-ray source) operating at a voltage of 40 kV and a current of 30 mA. UV-vis diffuse reflectance spectroscopy (DRS) spectra were measured by Shimadzu 3600 UV-vis-NIR spectrophotometer with an integrating sphere attachment. Photoluminescence (PL) spectra of the polymer powders were obtained using a FluoroLog-3 spectrofluorometer. Time-resolved fluorescent decays of the polymer powders were carried out on a Horiba DeltaFlex TCSPC system equipped with NanoLED (374 nm, 240 ps) pulsed excitation sources. The morphologies of the polymer powders were examined by field emission scanning electron microscopy (FE-SEM; JEOL JSM-7610F) at an acceleration voltage of 5 kV. Thermal gravimetric analyses (TGA) were performed on Schimadzu DTG-60AH thermal analyzer with a heating rate of 15 °C min^{-1} under N_2 atmosphere. Nitrogen and carbon dioxide adsorption and desorption were measured using a Micromeritics ASAP 2020 volumetric adsorption analyzer. Pore size distributions and pore volumes were derived from the adsorption branches of the isotherms using the non-local density functional theory (NL-DFT). Samples were degassed at 100 °C for 10 hours under vacuum before analysis.

Computational details

First-principles calculations were carried out using density functional theory (DFT) method as implemented in the Vienna ab initio simulation package (VASP).[1] The ion-electron interactions were treated with the projected augmented wave pseudopotentials,[2] and the general gradient approximation (GGA) with the Perdew-Burke-Ernzerhof functional was used to describe the exchange-correlation potential when performing geometric relaxations.[3] Hybrid functional of Heyd, Scuseria, and Ernzerhof (HSE06) were used for electronic structures calculations.[4] The

plane-wave basis was expanded up to a cut-off energy of 400 eV. All structures were relaxed using a conjugate gradient method until the residual force on every atom was less than 0.02 eV/Å, and the convergence criteria of total energy in the self-consistent field method was set to 10^{-5} eV. The adsorption energy of COOH* was calculated as follows:

$$E_{COOH*} = E_{[substrate + COOH]} - E_{[substrate]} - E_{[CO_2]} - \frac{1}{2} E_{[H_2]}$$

where $E_{[substrate + COOH]}$ and $E_{[substrate]}$ are the energies of substrates with and without adsorbates, respectively. $E_{[CO_2]}$ and $E_{[H_2]}$ are the energies of CO_2 and H_2, respectively. According to this definition, lower adsorption energy E means stronger adsorption, and vice versa.

Experimental details

Transient photocurrent response and electrochemical impedance spectroscopy (EIS) measurements. The photoelectrode was prepared by drop casting the polymers suspension (5 mg polymer mixed with 10 μL of 5 wt% Nafion) on the surface of a FTO glass and dried in air. The photoelectrode, Pt wire and Ag/AgCl were used as the working electrode, counter electrode, and reference electrode, respectively. The measurement was performed in 0.5 M Na_2SO_4 aqueous solution. Transit photocurrent response was measured using a 300 W Xenon lamp (MAX-302 xenon lamp, Asahi Spectra) with 420 nm cut off as the light source, while EIS plots were obtained in the dark. The applied bias potentials for both of the two measurements are +0.6 V (*vs*. Ag/AgCl).

Electrochemical measurements: Electrochemistry was conducted using a glassy carbon electrode coated polymer sample as the working electrode, a Ag/Ag^+ electrode as the reference electrode, and platinum plate as the counter electrode, and 0.1 M $TBAPF_6$ solution in acetonitrile

as the supporting electrolyte. The potential was recorded against ferrocene/ferrocenium (Fc/Fc^+). For the conversion from the Fc/Fc^+ redox couple to the normal hydrogen electrode (NHE), the equation $E_{NHE} = E_{Fc/Fc+} + 0.63$ V was applied.

Photocatalytic reduction of CO_2: The photocatalytic CO_2 reduction experiments were performed in a home-made glass reactor (100 mL) with a quartz window as reported in our previous work.[5] A 300 W Xe arc lamp (Newport 69907) was used as the visible light source with a long-pass cut-off filter (> 420 nm). 15 mg of photocatalyst was uniformly dispersed on the bottom of the reactor with a base area of 12 cm^2 and then dried at 150 ℃ for 2h. Pure CO_2 (99.99%) gas was passed through a water bubbler to provide a mixture of CO_2 and water vapor, which was purged into the reactor for 1h to drive away the air. The reaction temperature was kept at room temperature by cooling water. During light irradiation, the gas products were analyzed by Shimadzu GC 2010 Plus with a flame ionization detector (FID) and Agilent 7890A with a thermal conductive detector (TCD). No CO was detected in the absence of photocatalysts or light irradiation. While the reactor was purged with pure N_2 rather than CO_2, trace CO could be detected under light irradiation, indicating CO_2 is served as reductive agent in the system. No CO could be measured in the absence of water vapor, which indicates that H_2O plays an important role as an electron donor. Other products, such as HCOOH, HCHO, CH_3OH, were not detected. In addition, a small amount of O_2 was also detected for OXD-TPA in the photocatalytic system under visible light. To determine the source of the carbon in the product, isotopic experiments were conducted under the same conditions using $^{13}CO_2$ (purity: 99%), and the CO evolution was analyzed by gas chromatography-mass spectrometry (GC-MS).

Quantum efficiency: The quantum efficiency (QE) of polymer for CO_2 photoreduction reaction was evaluated under visible light irradiation for 3 h using a band-pass filter. The light source is

300 W Xe arc lamp (Newport 69907) and the illumination area is 12 cm^2. Assume that the incident photons are all absorbed by the sample. The QE was calculated according to equation below:

$$\text{QE}\ (\%) = \frac{Number\ of\ reacted\ electrons}{Number\ of\ incident\ photons} \times 100\%$$

$$= \frac{2 \times Number\ of\ evolved\ CO\ molecules}{Number\ of\ incident\ photons} \times 100\%$$

$$= \frac{2 \times N \times N_A}{S \times E \times t \times \lambda/(h \times C)} \times 100\%$$

$$= \frac{2 \times N \times N_A \times h \times C}{S \times E \times t \times \lambda} \times 100\%$$

where N is the amount of the evolved CO gas (mol); N_A is the Avogadro constant (6.023×10^{23} mol^{-1}); *h* is the Planck constant (6.626×10^{-34} J·s); C is the velocity of light in vacuum (3×10^8 m s^{-1}); S is the irradiation area; E is incident monochromatic light intensity (W cm^{-2}); t is the light irradiation time (s); λ is the monochromatic light wavelength (m). The monochromatic focused intensity at 420, 450, 500, 550 and 600 nm measured by a digital handheld optical power and energy meter console (PM100D, Thorlabs GmbH, Germany). The FWHM is all 40 nm.

Synthesis of the monomers and polymers

The monomer tris(4-ethynylphenyl)amine,[6] 2,5-bis(4-bromophenyl)-1,3,4-oxadiazole,[7] were synthesized by following in the literatures with slight modifications. The synthetic route of conjugated microporous polymers is shown in Scheme S1 and the detailed synthetic procedures are described as follows. 4,4-Dibromobiphenyl was further purified by recrystallization before polymerization.

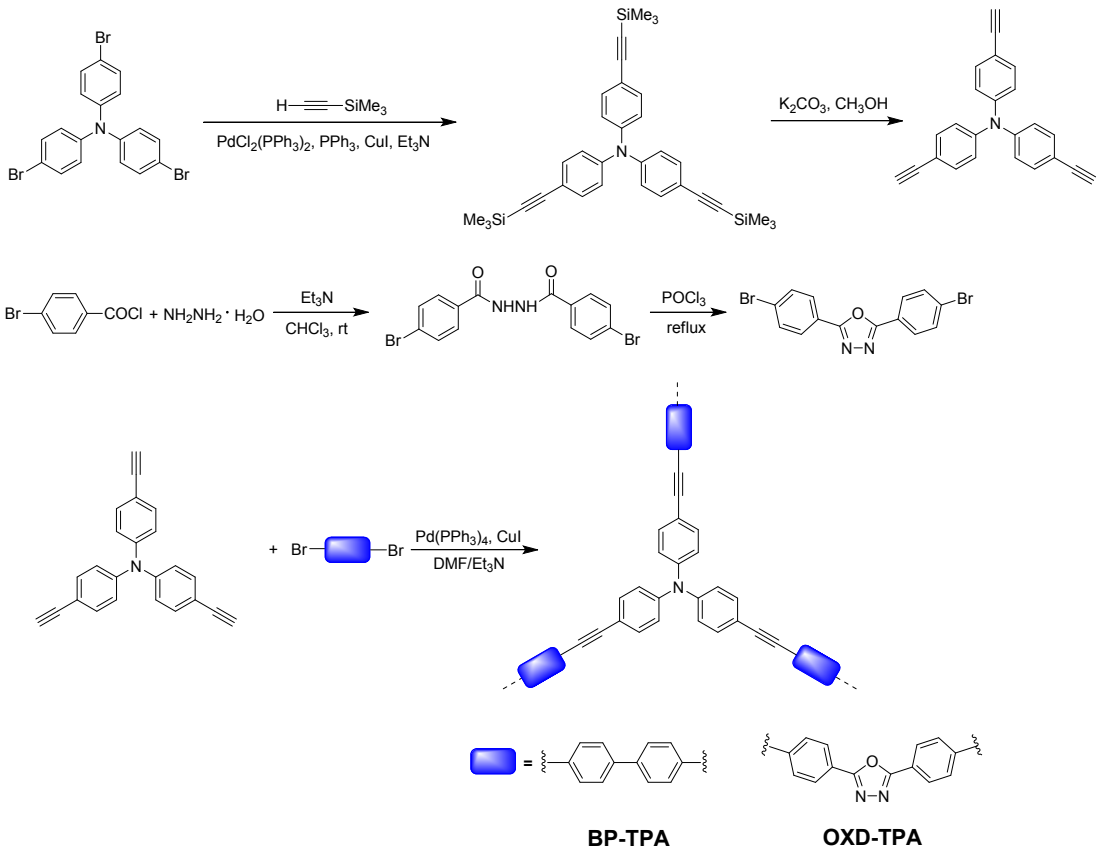

Scheme S1. Synthesis of the monomers and conjugated microporous polymers in this study.

General procedure for the synthesis of conjugated microporous polymers: All polymerization reactions were carried out with similar monomer concentration and a fixed reaction temperature and reaction time. Tris(4-ethynylphenyl)amine (158.7 mg, 0.50 mmol), dibormosubstituted monomer (0.75 mmol), $Pd(PPh_3)_4$ (15 mg), and CuI (5 mg) were dissolved in a mixture of anhydrous DMF (3 mL) and Et_3N (3 mL). The reaction mixture was heated to 100 ℃ and stirred for 48 h. After cooling to room temperature, the mixture was poured into water and filtered. The insoluble polymer powder was washed with water, methanol, and acetone to remove any low-molecular polymers or catalyst residues. Further purification of the polymer was carried out by Soxhlet extraction with THF and $CHCl_3$ successively for 24 h each. The product was then dried under vacuum for 24 h at 100 ℃ to give final product.

BP-TPA: yellow powder, 248 mg. Yield: 91%. Anal. Calcd for $(C_{60}H_{39}N)_n$: C, 93.11; H, 5.08; N, 1.81%; Found C, 89.28; H, 3.39; N, 2.04%; Pd, 0.34%; Cu, 0.017%.

OXD-TPA: yellow powder, 301 mg. Yield: 93%. Anal. Calcd for $(C_{66}H_{39}N_7O_3)_n$: C, 81.05; H, 4.02; N, 10.02; Found C, 75.21; H, 1.59; N, 6.85%; Pd, 0.54%; Cu, 0.025%.

ESI 3. Solid state ^{13}C NMR spectra of the polymers

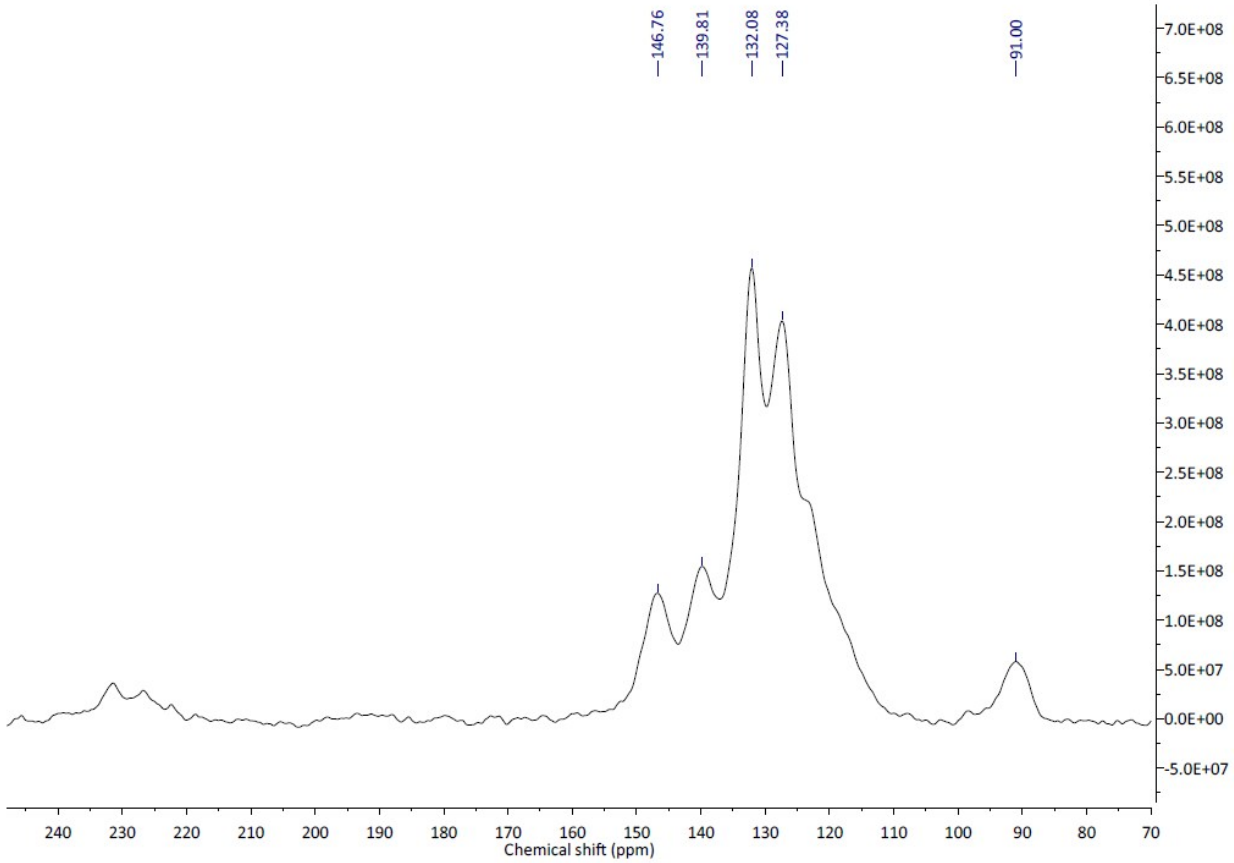

Figure S1. ^{13}C CP/MAS solid-state NMR spectrum of BP-TPA.

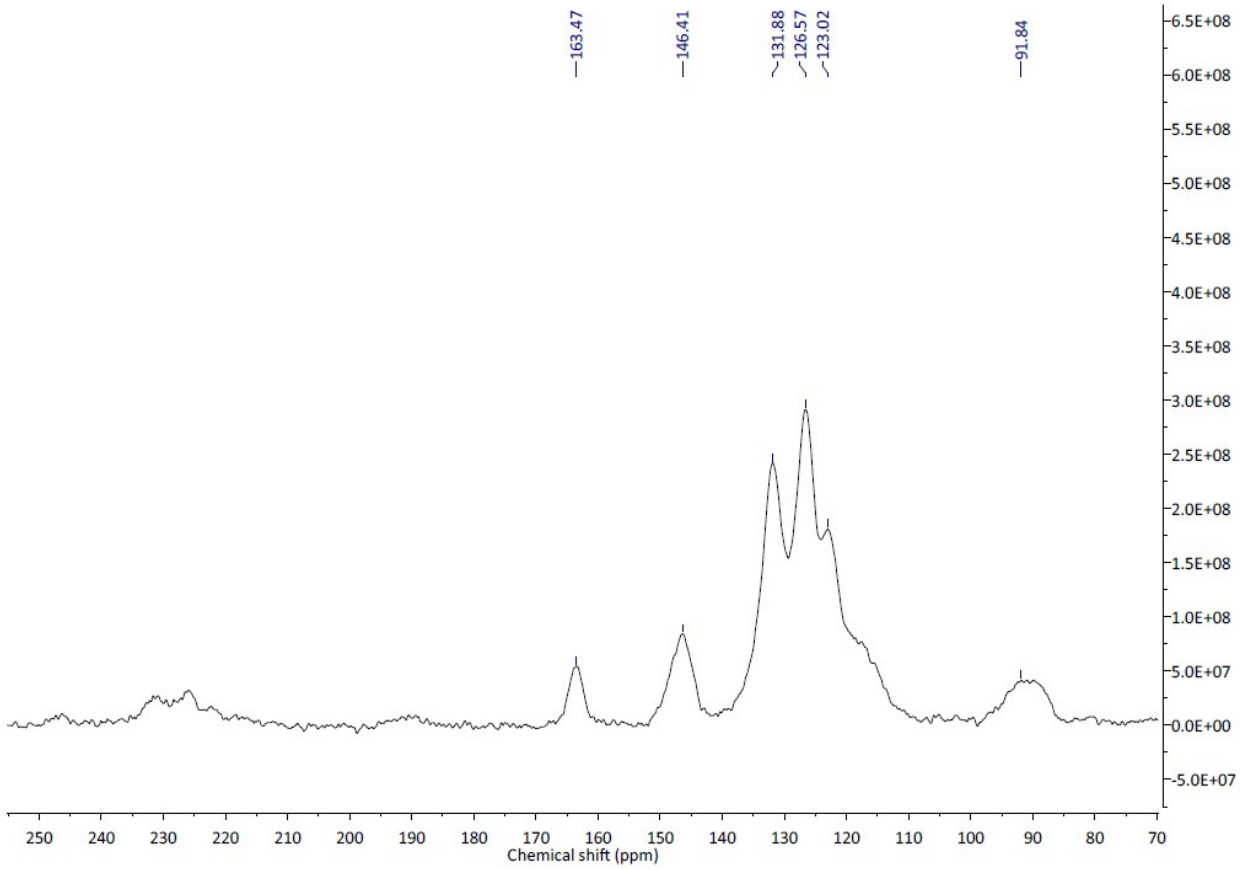

Figure S2. ^{13}C CP/MAS solid-state NMR spectrum of OXD-TPA.

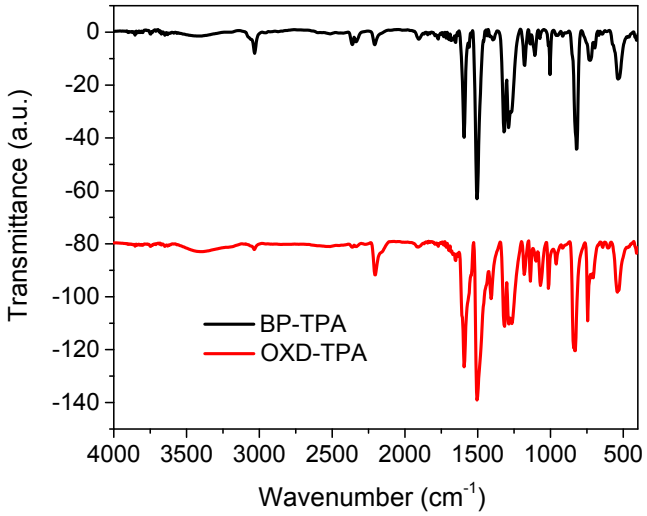

Figure S3. FTIR spectra of BP-TPA and OXD-TPA.

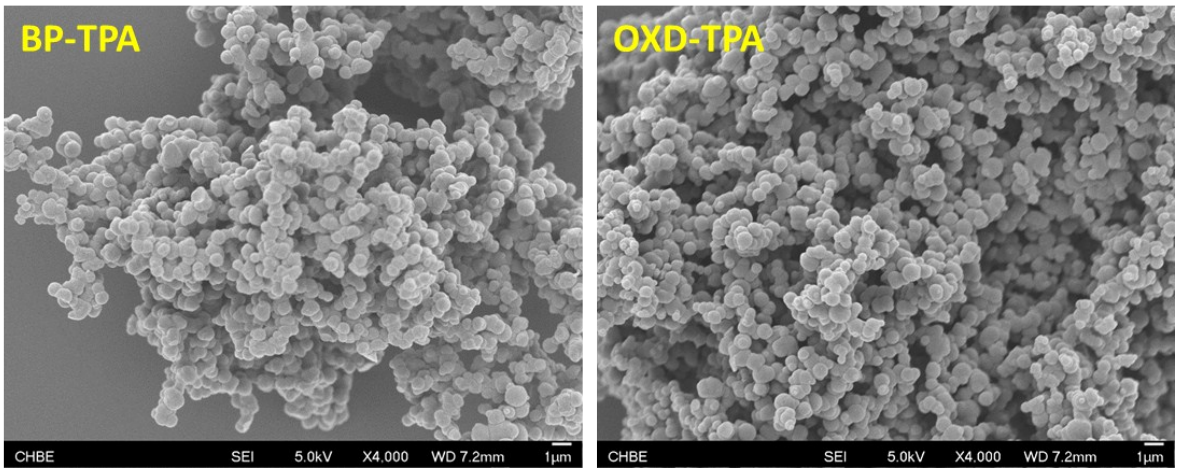

Figure S4. SEM images of BP-TPA and OXD-TPA.

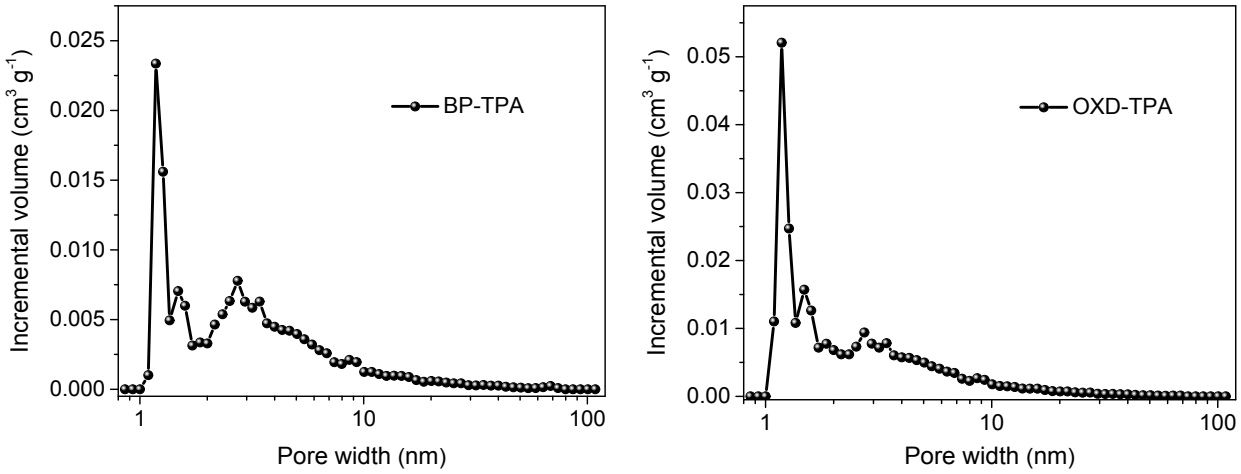

Figure S5. Pore size distribution of BP-TPA and OXD-TPA.

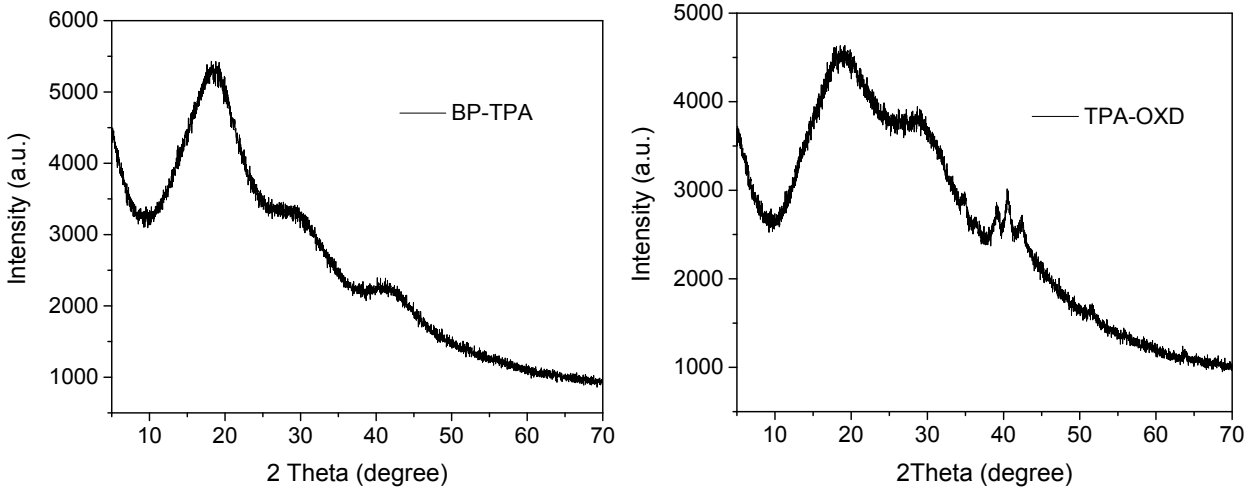

Figure S6. Powder X-ray diffraction (PXRD) patterns of BP-TPA and OXD-TPA.

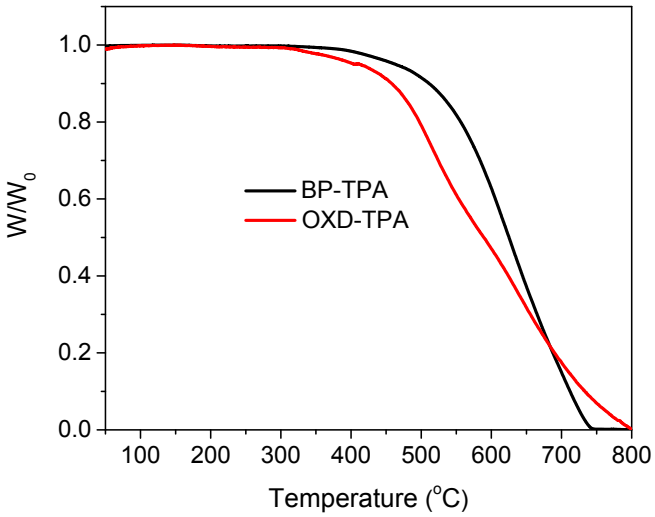

Figure S7. Thermogravimetric analysis (TGA) curves for BP-TPA and OXD-TPA, recorded under nitrogen at a heating rate of 15 ^{o}C min^{-1}.

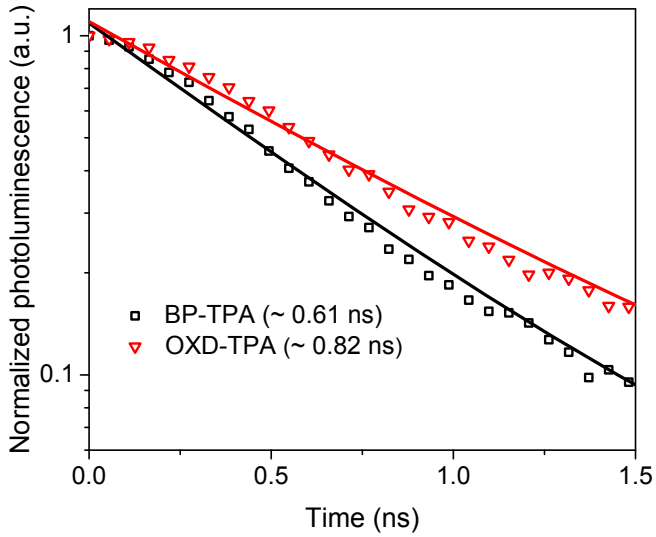

Figure S8. Time-resolved photoluminescence spectra of as-prepared polymer powders measured by time-correlated single-photon counting (excited at 380 nm).

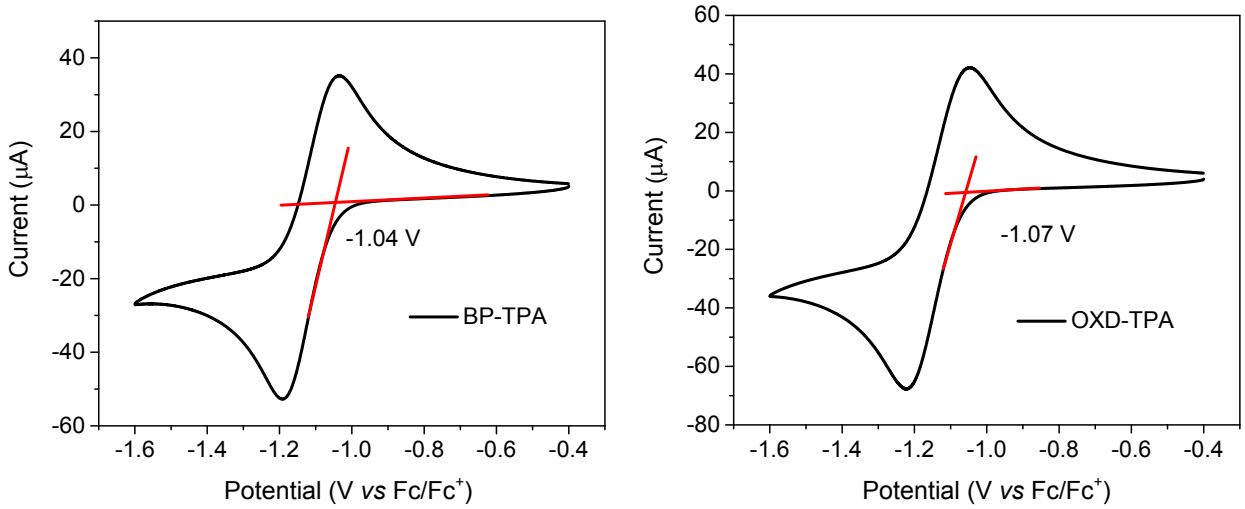

Figure S9. Cyclic voltammograms curves of BP-TPA and OXD-TPA in deoxygenated anhydrous CH_3CN solution of $TBPAF_6$ (0.1 M) and Fc (20.0 mM).

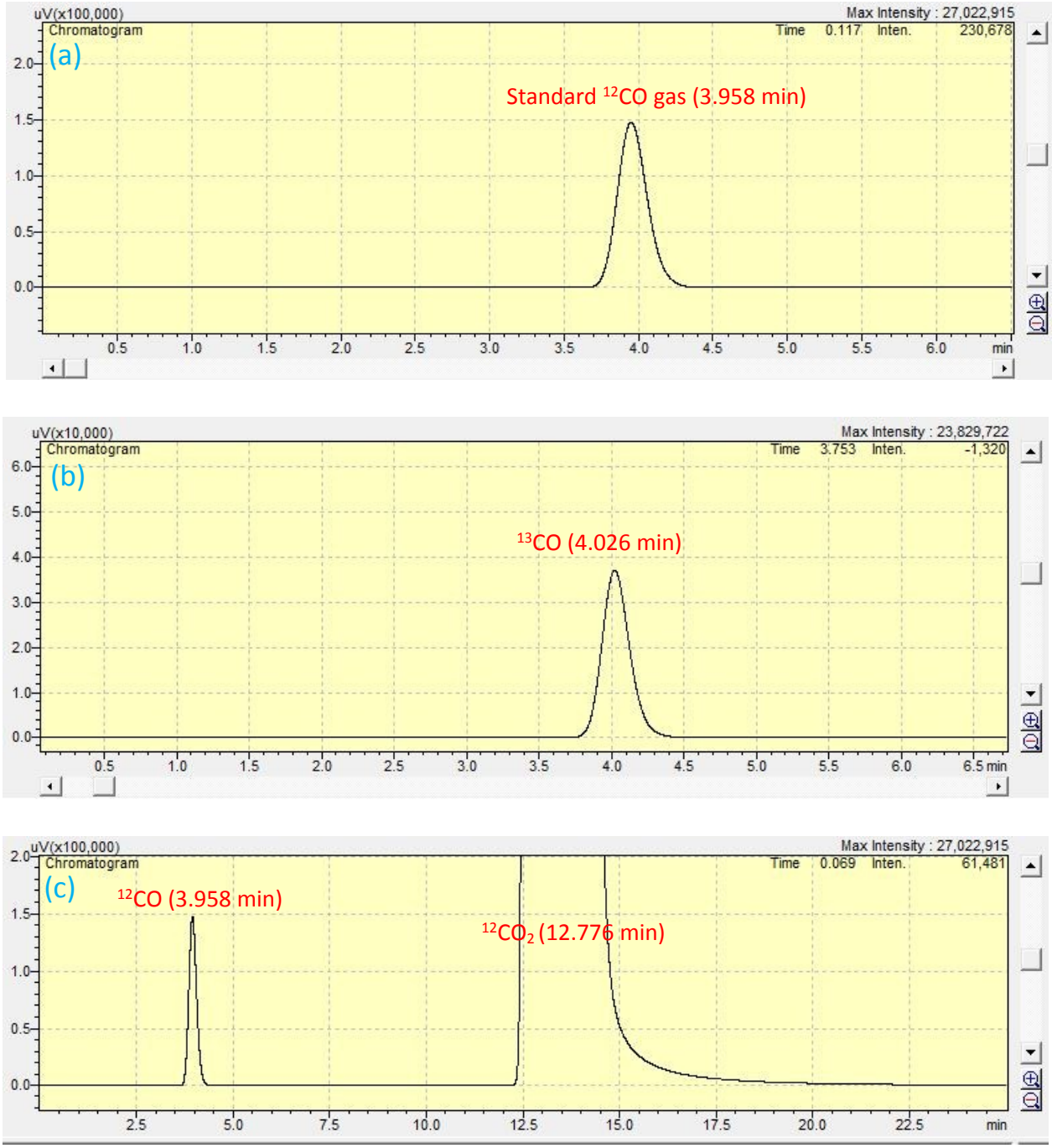

Figure S10. Gas chromatograph of (a) standard CO gas and (b) ^{13}CO from photoreduction of $^{13}CO_2$ by OXD-TPA under visible light irradiation; (c) gas chromatograph trace of evolved CO (15 mg OXD-TPA after 5h photocatalytic reaction).

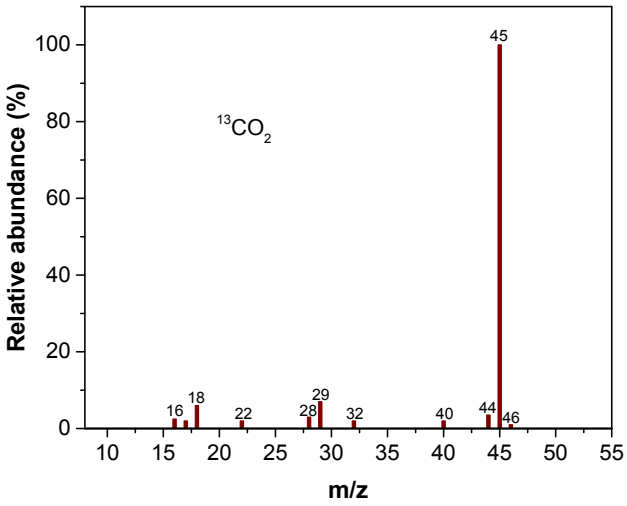

Figure S11. Mass spectrum of pure $^{13}CO_2$ (m/z = 45).

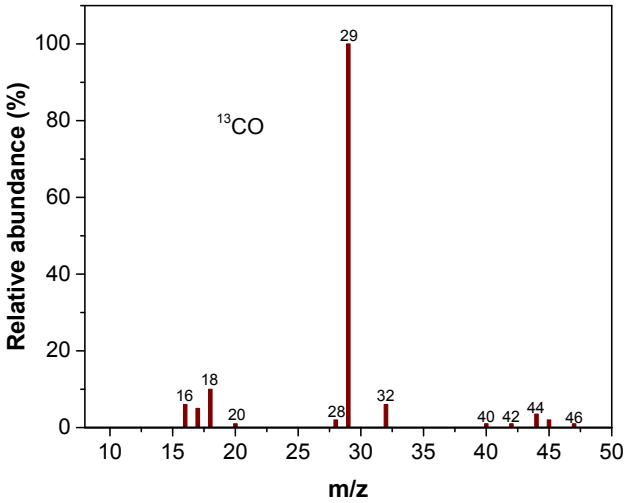

Figure S12. (a) Total ion chromatogram and (b) mass spectrum of generated ^{13}CO from photoreduction of $^{13}CO_2$ by OXD-TPA under visible light irradiation. *m/z* = 18 and *m/z* = 29 are assigned to H_2O and ^{13}CO, respectively. Concentrated NaOH aqueous solution were added to remove unreacted $^{13}CO_2$ in the reactor after photocatalytic reaction.

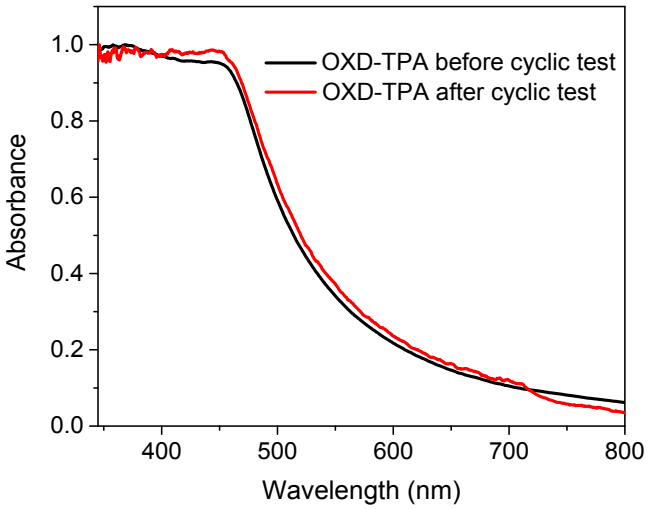

Figure S13. UV-vis diffusion reflectance spectra of OXD-TPA before and after cyclic test.

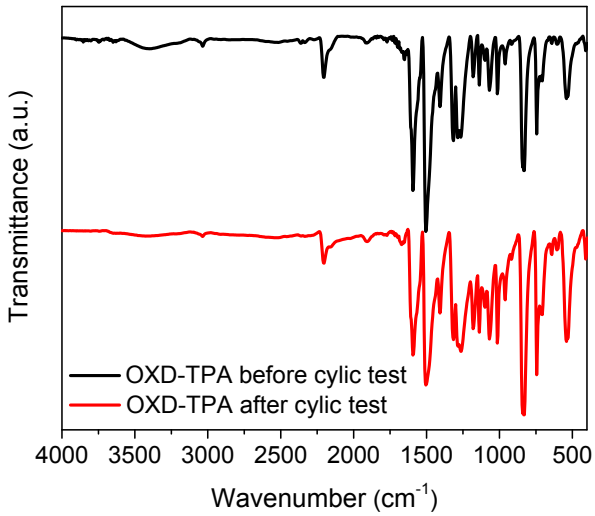

Figure S14. FTIR spectra of OXD-TPA before and after cyclic test under visible light irradiation.

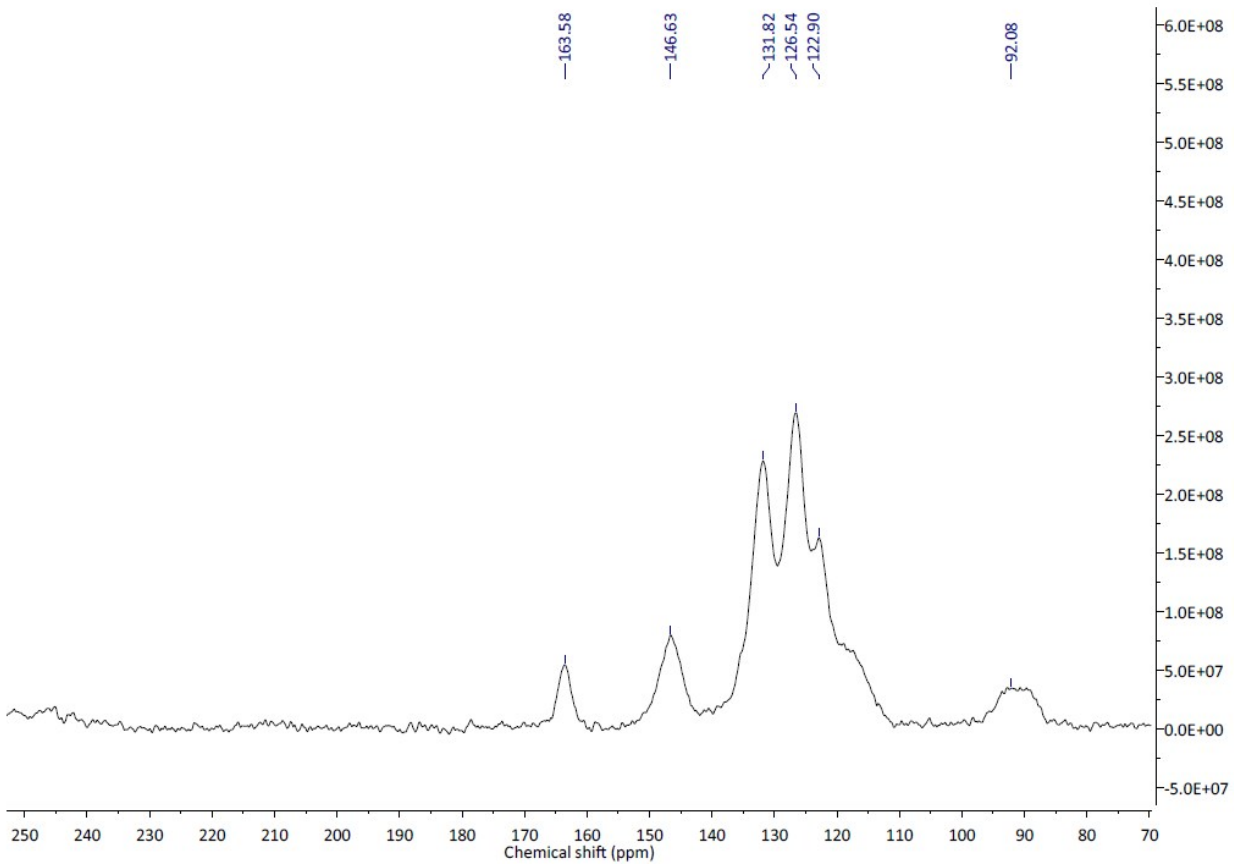

Figure S15. ^{13}C CP MAS NMR of OXD-TPA after cyclic test.

Table S1. Recent reports of CO_2 photoreduction in gas-solid systems based on C_3N_4 and porous conjugated polymers under visible light irradiation (> 420 nm).

Light source	catalysts	cocatalyst	main products and highest efficiency[a]	Reference
300 W Xe lamp	g-C_3N_4/$NaNbO_3$ Heterojunction	Pt	CH_4: 6.4 μmol h^{-1} g^{-1}	*ACS Catal.* **2014**, *4*, 3637
300 W Xe lamp	g-C_3N_4/Bi_2WO_6	---	CO: 5.19 mmol g^{-1} h^{-1}	*J. Mater. Chem. A,* **2015**, *3*, 5189
300 W Xe Lamp	g-C_3N_4/SnS_2 heterojunction	---	CH_4: 0.64 μmol h^{-1} g^{-1} CH_3OH: 2.24 μmol h^{-1} g^{-1}	*J. Catal.* **2017**, *352*, 532
350 W Xe lamp	O-Doped g-C_3N_4	---	CH_3OH: 0.88 μmol h^{-1} g^{-1}	*Small* **2017**, *13*, 1603938
300 W Xe lamp	α-Fe_2O_3/g-C_3N_4	---	CO: 27.2 μmol h^{-1} g^{-1}	*Adv. Mater.* **2018**, *30*, 1706108
300 W Xe lamp	Porous conjugated polymers	---	CO: 33 μmol h^{-1} g^{-1} H_2: 5 μmol h^{-1} g^{-1}	*Angew. Chem. Int. Ed.* **2019**, *58*, 632
300 W Xe lamp	Porous conjugated polymers	---	CO: 37.15 μmol h^{-1} g^{-1}	**This work**

a) The values are calculated according to the reported data in literatures.

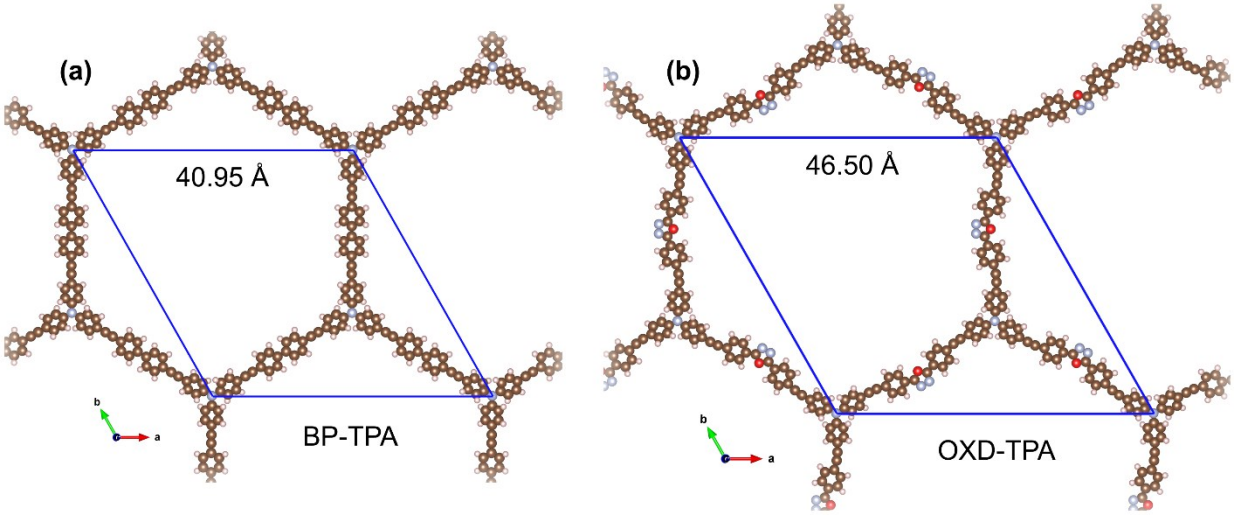

Figure S16. Optimized structures of the model BP-TPA and OXD-TPA in DFT calculations.

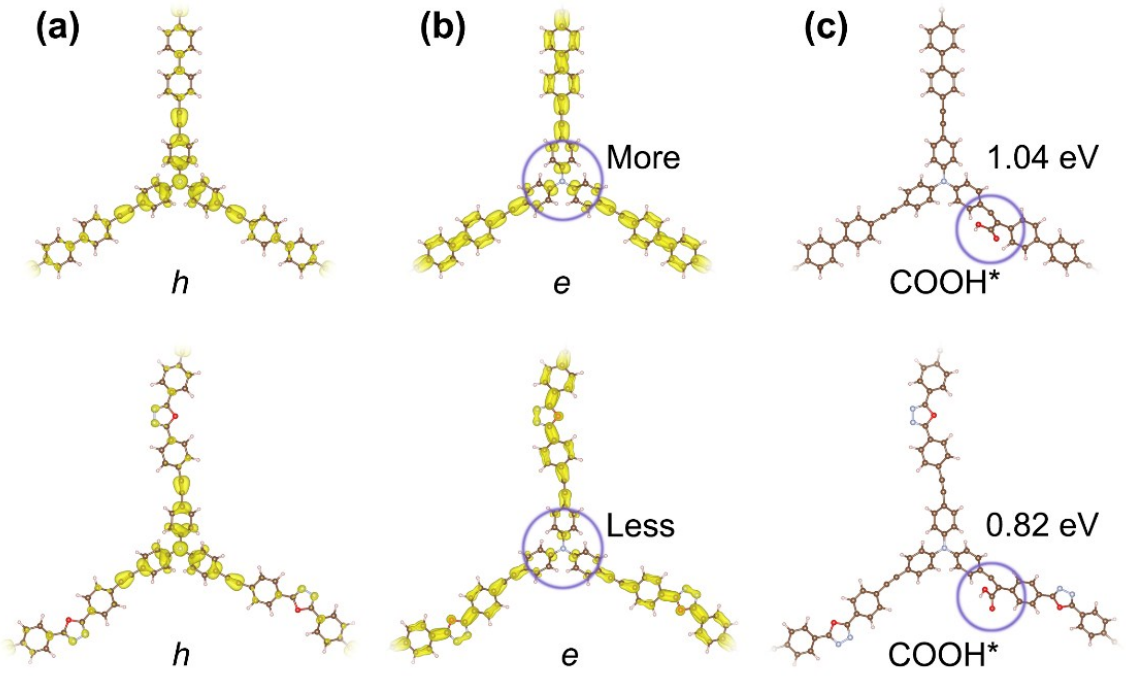

Figure S17. (a) Excited-state hole distribution (0.001 e/bohr^3), (b) excited-state electron distribution (0.001 e/bohr^3), and (c) optimized intermediate COOH* for BP-TPA and OXD-TPA.

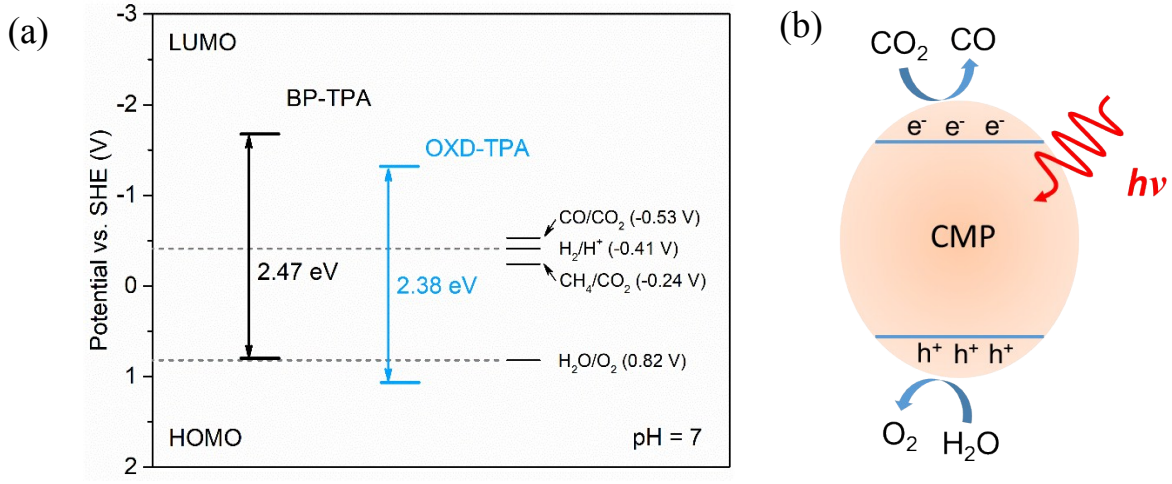

Figure S18. (a) Hybrid DFT calculated potentials of frontier orbitals and electronic bandgaps in model BP-TPA and OXD-TPA. (b) Possible mechanism for CO_2 photoreduction over TPA based conjugated microporous polymers in this study. Following the absorption and activation of CO_2 by the porous polymer, the photoinduced holes was utilized for oxidize water to generate oxygen and hydrogen ions *via* the half-reaction ($2H_2O + 4h^+ \rightarrow O_2 + 4H^+$), while the generated electron was used to reduce CO_2 to CO ($CO_2 + 2H^+ + 2e^- \rightarrow CO + H_2O$).

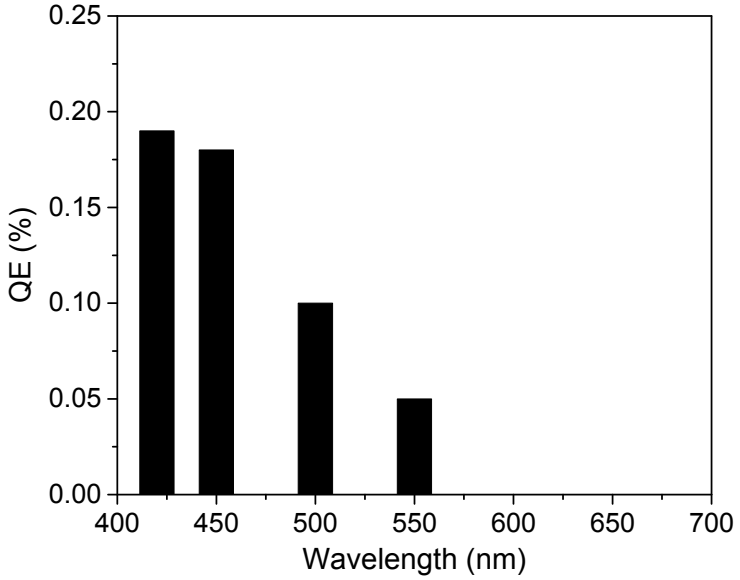

Figure S19. Wavelength-specific quantum efficiency of OXD-TPA using 40 nm FWHM band-pass filters.

References

(1) G. Kresse, J. Furthmüller, *Phys. Rev. B* **1996**, *54*, 11169.

(2) P. E. Blochl, *Phys. Rev. B* **1994**, *50*, 17953.

(3) J. P. Perdew, K. Burke, M. Ernzerhof, *Phys. Rev. Lett.* **1996**, *77*, 3865.

(4) J. Heyd, G. E. Scuseria, M. Ernzerhof, *J. Chem. Phys.* **2003**, *118*, 8207.

(5) Y. Liao, S. Cao, Y. Yuan, Q. Gu, Z. Zhang, C. Xue, *Chem. Eur. J.* **2014**, *20*, 10220.

(6) Z. Xie, Y. Wei, X. Zhao, Y. Li, S. Ding, Long Chen, *Mater. Chem. Front.* **2017**, *1*, 867.

(7) W.-Y. Wong, Y.-H. Guo, *J. Mol. Struct.* **2008**, *890*, 150.